Construction of Defect-Diminished Lithium 10,12-Heptacosadiynoate Monolayer by Means of Crystallization on the Water Surface

Keisuke KURIYAMA and Tisato KAJIYAMA*
Department of Chemical Science and Technology, Faculty of Engineering, Kyushu University,
6-10-1 Hakozaki, Higashi-ku, Fukuoka 812

(Received April 15, 1993)

The melting temperature, T_m of lithium 10,12-heptacosadiynoate monolayer on the water surface was evaluated by a combination of two kinds of measurements, the subphase temperature, T_{sp} dependence of modulus of the monolayer based on a π–A isotherm and also, the T_{sp} dependence of the electron diffraction, ED patterns of the monolayer. T_m of the monolayer was evaluated to be 300 K from the results of both an apparent decrease in the T_{sp} vs. modulus curve and the change of the ED pattern from a crystalline triclinic spot to an amorphous halo. The aggregation structure of the monolayer during a compressing process at T_{sp} below and above T_m was investigated on the basis of the bright field electron micrograph and the ED pattern. The monolayer on the water surface was classified into a crystalline monolayer and an amorphous one depending on the T_{sp} below and above T_m of the monolayer, respectively. However, the formation of the crystalline and amorphous monolayers is irrespective of the surface pressure. Furthermore, the defect-diminished crystallized monolayer was prepared by cooling the amorphous monolayer down to a temperature range below T_m.

Conjugated polymers have attracted enormous attention because of their strong third order optical nonlinearity. In particular, polydiacetylenes (PDAs) are well-known to have a relatively large third order nonlinear optical susceptibility, $\chi^{(3)}$ and extensively studied for their practical applications such as optical switching, nonlinear memory, and optical waveguide.[1] However, the magnitude of $\chi^{(3)}$ for PDAs is not enough for all optical devices at the present time. The magnitude of $\chi^{(3)}$ for conjugated polymers such as PDAs is strongly dependent on the delocalization length of π-electron.[2—4] In order to make the magnitude of $\chi^{(3)}$ increase, PDA with longer delocalization length of π-electron is desired. PDA can be obtained by the solid state (topochemical) polymerization of diacetylene monomer single crystal.[5] Therefore, higher ordered large monomer single crystal is required to obtain PDA with longer delocalization length of π-electron along a polymer main chain. Moreover, for applications to integrated optical devices, PDA molecules must be assembled into thin films. In these points, the monolayer of diynoic acid on the water surface has been enthusiastically suited because of its ability to form a large two-dimensional single crystal with crystallographically superior quality.[6]

In recent years, many studies have been carried out on both the polymerization process and the photoreactivity of Langmuir–Blodgett (LB) films of various diacetylene derivatives.[7—11] It was reported from these studies that the polymerization process and the photoreactivity of diacetylene derivatives were strongly affected by the relative position of adjacent 1,3-butadiyne-1,4-diyl groups. Thus, the aggregation structure of monomer monolayer of diacetylene derivatives is an important factor of its polymerization. For the construction of PDA monolayer with longer delocalization length of π-electron, the defect-diminished monomer monolayer in which the 1,3-butadiyne-1,4-diyl groups are well arranged is required. The authors have reported that the defect-diminished monolayer can be prepared by the cooling-crystallization method, which is strongly related to thermal molecular motions of the monolayer on the water surface.[6] Also, the melting temperatures (T_ms) and the crystalline relaxation temperatures ($T_{\alpha c}$s) of the fatty acid monolayers on the water surface were evaluated, because the thermal behaviors of the monolayers on the water surface are very important for the investigation of the aggregation structure of the monolayers.[12]

In this paper, the melting temperature (T_m) of lithium 10,12-heptacosadiynoate monolayer on the water surface was evaluated from the subphase temperature (T_{sp}) dependences of both the modulus and the electron diffraction (ED) pattern of the monolayer. The aggregation structure of the monolayer during a compressing process at T_{sp} below and above T_m was also investigated on the basis of the bright field electron micrograph and the ED pattern. Furthermore, as a precursor of PDA with longer delocalization length of π-electron, the defect-diminished crystallized monolayer was constructed by cooling the amorphous monolayer down to a temperature region below T_m.

Experimental

Monolayer Preparation. 10,12-Heptacosadiynoic acid (chromatographic reference quality) was used without further purification. Benzene with spectroscopic quality was used as a spreading solvent. A benzene solution of 10,12-heptacosadiynoic acid was prepared with the concentration of 2.0×10^{-3} mol L^{-1}. The subphase water was purified by a Milli-QII system (Millipore Co., Ltd.). The trough dimensions were $502\times150\times5$ mm. The subphase temperature, T_{sp} was varied in a temperature range of 283—308 K by circulating constant-temperature water around the aluminum support of the trough. The control accuracy of T_{sp} was ±1 K which was evaluated by using a thermocouple positioned ca. 1 mm below the water surface. The monolayer was prepared by spreading the benzene solution of 10,12-heptacosadiynoic acid on the water subphase containing 2.0×10^{-3} mol L^{-1} of LiOH.[13,14] Monolayer was compressed to a given surface pressure at the area change rate of 2×10^{-3}nm^2 molecule^{-1} s^{-1}.

Modulus Measurement of Monolayer. Π–A isotherms were obtained at various T_{sp}s with a microprocessor-controlled film balance system (FSD-20, Sanesu Keisoku Co., Ltd.). The static elasticity, K_s of the monolayer on the water surface was evaluated from the π–A isotherm by using the following equation.[15,16)]

$$K_s = -A(d\pi/dA)$$

In this paper, the temperature dependence of the maximum of log K_s, log $K_{s(max)}$, was adopted for determination of the T_m of the lithium 10,12-heptacosadiynoate monolayer on the water surface, because log $K_{s(max)}$ was observed when 10,12-heptacosadiynoic acid molecules in the monolayer were packed most densely and therefore, homogeneous compression force was thought to be transmitted throughout the monolayer.

Substrate Preparation. The hydrophilic SiO substrate (static water contact angle=30°) was prepared by vapor-deposition of SiO onto a Formvar-covered electron microscope grid (200-mesh) for electron microscopic observations. The hydrophilic SiO substrate is suitable for the electron microscopic morphological and structural investigation for the lithium 10,12-heptacosadiynoate monolayer on the water surface, since the crystal system of the monolayer on the water surface is stably maintained on the hydrophilic SiO substrate upon transferring the monolayer by the upward drawing method.[12,17] This is because the hydrophilic group of acid molecule contacts with the hydrophilic substrate and this situation of monolayer–substrate interface is similar to that of monolayer–water interface with respect to the magnitude of interfacial free energy between the hydrophilic group and the substrate. Also, the surface of hydrophilic SiO substrate was confirmed to be smooth and amorphous, based on morphological and ED studies, respectively. Then in this study, the monolayer was transferred onto the hydrophilic SiO substrate by the upward drawing method at a transfer rate of 100 mm min^{-1} at various T_{sp}s and pressures, except at the surface pressure of 0 mN m^{-1}. The monolayer at 0 mN m^{-1} could be transferred only by a horizontal lifting method.[18,19]

Electron Microscopic Observation. Bright field electron micrographs and ED patterns were taken with a Hitachi H-7000 electron microscope, which was operated at an acceleration voltage of 75 kV and a beam current of 0.5 μA. The electron beam was 2 μm in diameter. Electron microscopic observations were carried out at the same temperature with T_{sp} at which the monolayer was prepared on the water surface, by using a cryotransfer system (Gatan Co., Ltd.). Pt–carbon was vapor-deposited onto the monolayer samples with a shadowing angle of 23° in order to obtain a distinct contrast for the bright field electron microscopic observations.

Evaluation of Crystallographical Quality of Monolayer. Crystallographical quality of the monolayer was evaluated in terms of the magnitude of crystallographical distortion and continuity in a direction along the monolayer surface, that is, the *hk*0 direction. Crystallographical distortion and continuity correspond to the route mean square value of differential rate between the positions of ideal crystalline lattice and real crystalline lattice, and the crystalline lattice length contributing to the electron diffraction coherently, respectively. These values were quantitatively evaluated by a modified single line method based on the Fourier analysis of ED profiles.[20] As a reference, high density polyethylene single crystal was prepared under suitable conditions of crystallization.

Results and Discussion

Determination of Melting Temperature of the Monolayer on the Water Surface. Figure 1 shows the T_{sp} dependence of log $K_{s(max)}$ for the lithium 10,12-heptacosadiynoate monolayer on the water surface and also, ED patterns of the monolayer transferred onto the hydrophilic substrates at the surface pressure of 20 mN m^{-1}, at which the lithium 10,12-heptacosadiynoate monolayer was confirmed to be morphologically homogeneous. The ED patterns were taken at the same temperature as T_{sp} at which the monolayer was formed. With an increase in T_{sp}, the magnitude of log $K_{s(max)}$ increased and started to decrease at around 293 K. The ED patterns at 298 and 303 K were a crystalline Debye ring and an amorphous halo, respectively. Therefore, it is apparent from Fig. 1 that the monolayer on the water surface melts in a temperature region above 298 K. On the other hand, in a low temperature region below 293 K, the magnitude of log $K_{s(max)}$ decreased with a decrease in T_{sp}, and the monolayer on the water surface was in an amorphous state at 283 and 288 K as shown by the ED patterns. This may indicate that the monolayer at T_{sp} below 288 K is in a glassy state, because lithium 10,12-heptacosadiynoate molecules are quenched maintaining the conformational misalignment along a hydrocarbon chain owing to strikingly fast evaporation of solvent. In order to clarify this quench effect for the monolayer on the water surface, the T_{sp} dependences of both log $K_{s(max)}$ and ED pattern were investigated by using the monolayer prepared by cooling the amorphous monolayer down to T_{sp} of 283 K from T_{sp} of 303 K at the cooling rate of 15 K h^{-1} and also, at a surface pressure of 12 mN m^{-1}.

Figure 2 shows the T_{sp} dependences of log $K_{s(max)}$ and ED pattern of the monolayer prepared by the process mentioned above. This monolayer preparation corresponds to the case without a quench effect, because the amorphous monolayer was slowly cooled down to the temperature of 283 K. The ED pattern at 283 K exhibited a crystalline triclinic spot which was apparently different from the ED pattern of an amorphous halo, as shown in Fig. 1. The magnitude of log $K_{s(max)}$ started to decrease apparently at ca. 300 K without any expression of the maximum log $K_{s(max)}$. Since the ED patterns at 298 and 303 K were a crystalline tri-

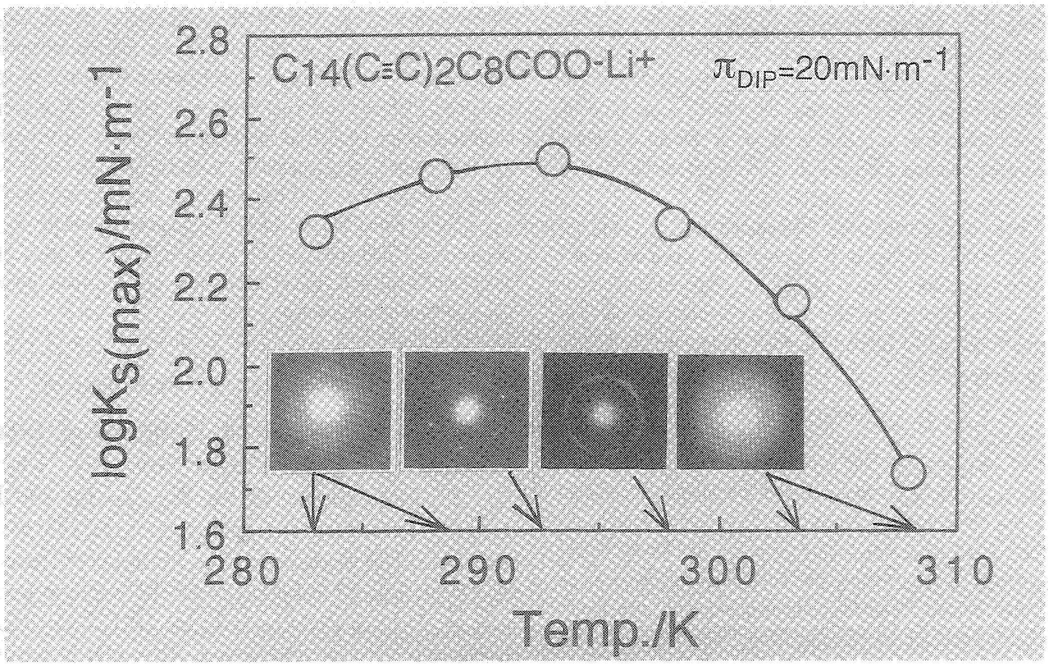

Fig. 1. T_{sp} dependence of log $K_{\mathrm{s(max)}}$ and ED patterns of lithium heptacosadiynoate monolayer.

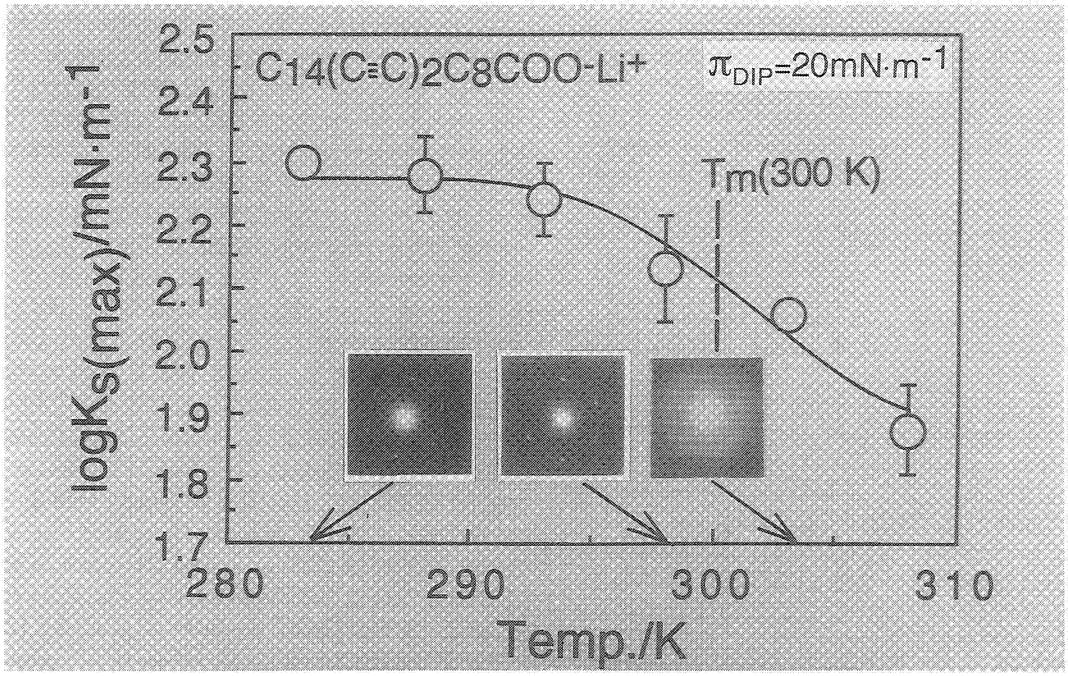

Fig. 2. T_{sp} dependence of log $K_{\mathrm{s(max)}}$ and ED patterns of lithium heptacosadiynoate monolayer without quench effect.

clinic spot and an amorphous halo, respectively, T_{m} of lithium 10,12-heptacosadiynoate monolayer on the water surface was evaluated to be around 300 K. T_{m} of the monolayer on the water surface is much lower than that of three-dimensional crystal of 10,12-heptacosadiynoic acid ($T_{\mathrm{m}}=342$ K). This is reasonable, because the monolayer is thermodynamically less stable than its three-dimensional crystal.

The Aggregation Structure of Monolayer during a Compressing Process at T_{sp} below and above T_{m}. Figure 3 shows the π–A isotherm at T_{sp} of 283 K which was much lower than T_{m} of the monolayer and also, the bright field images and the ED patterns of the monolayers being transferred onto the hydrophilic SiO substrate at surface pressures of 0 and 17 mN m^{-1}. The π–A isotherm showed a steep rise of surface pressure with decreasing surface area without any plateau region. At 0 mN m^{-1}, many isolated domains were observed in the bright field image, as shown by an inserted photograph in Fig. 3. The bright field image of the monolayer at 17 mN m^{-1} exhibited the fairly uniform, smooth and continuous morphology. The ED

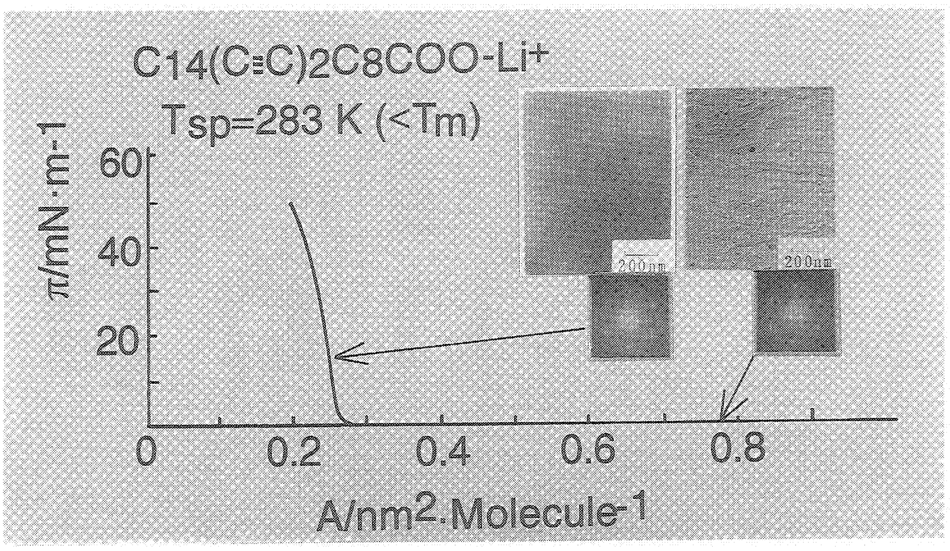

Fig. 3. Π–A isotherm, electron micrographs and ED patterns of lithium heptacosadiynoate monolayer at $T_{\rm sp}$ of 283 K.

patterns of the monolayer being transferred onto the substrate at 0 and 17 mN m^{-1} exhibited a crystalline triclinic spot. The distinctly sharp ED spot indicates that the dimension of crystalline domains is fairly large in comparison with an electron beam diameter of 2 μm, even at a surface pressure of 0 mN m^{-1}. Also, the ED pattern makes us expect that a large area monodomain monolayer may be formed due to a sintering or fusion at the interfaces among the domains during a continuous compression on the water surface.[21)]

Figure 4 shows the π–A isotherm for the monolayer at $T_{\rm sp}$ of 303 K above $T_{\rm m}$ of the monolayer, together with the bright field images and the ED patterns of the monolayer being transferred on the hydrophilic SiO substrate at 0, 5, and 20 mN m^{-1}. A plateau region on the π–A isotherm was observed in a surface area range of 0.50—0.30 nm^2 molecule^{-1}. At 0 mN m^{-1}, many isolated domains with round shape were observed in the bright field image. The bright field images showed that morphology of the monolayer became uniform with increasing surface pressure. The ED patterns were amorphous halos, being irrespective of the surface pressure. Therefore, Fig. 4 indicates that amorphous domains being formed already at 0 mN m^{-1} are aggregating during a continuous surface compression, without any phase transition such as the one from an amorphous phase to a crystalline phase.

Figures 5(a) and 5(b) show the schematic representations for the aggregation structure of lithium 10,12-heptacosadiynoate monolayers at $T_{\rm sp}$ below and above $T_{\rm m}$, respectively. On the basis of the morphologically structural studies mentioned above, the monolayer on the water surface is classified into a crystalline monolayer and an amorphous one depending on $T_{\rm sp}$ below and above $T_{\rm m}$ of the monolayer, respectively. In the case of $T_{\rm sp}$ below $T_{\rm m}$ (Fig. 5(a)), there is no plateau region on the π–A isotherm. The isolated two-dimensional crystalline domains are formed on the water surface at 0 mN m^{-1}. During compression on the water surface, these crystalline domains aggregate, resulting in the formation of a morphologically homogeneous monolayer. This type of monolayer was designated the crystalline monolayer.[12,22)] In the case of $T_{\rm sp}$ above $T_{\rm m}$ (Fig. 5(b)), there is a plateau region on a π–A isotherm. Many gel-type domains, in which lithium 10,12-heptacosadiynoate molecules aggregate randomly on the water surface, are formed in a low surface pressure region. With an increase in surface pressure, the amorphous domains aggregate, resulting in the formation of a morphologically homogeneous monolayer. This type of monolayer was designated the amorphous monolayer.[12,22)] It seems reasonable to consider that there is no apparent boundary surfaces (interface) among the amorphous domains in the aggregated homogeneous state due to gel-like interface. Therefore, the amorphous monolayer is thought to be in a more homogeneous state on a microscopic level rather than the crystalline monolayer. It is apparently expected that a large two-dimensional single crystal with a small number of defect can be prepared by cooling-crystallization of the amorphous monolayer.

Construction of Defect-Diminished Crystallized Monolayer of Lithium 10,12-Heptacosadiynoate. Figure 6 shows the preparation process for the crystallized monolayer of lithium 10,12-heptacosadiynoate. The amorphous monolayer was prepared on the water surface at $T_{\rm sp}$ of 303 K above $T_{\rm m}$ (ca. 300 K) and then, was compressed to the surface pressure of 12 mN m^{-1}. With maintaining this surface pressure, $T_{\rm sp}$ was reduced to the temperature of 283 K below $T_{\rm m}$ with the cooling speed of 15 K h^{-1} and finally, the monolayer was further crystallized for 20 min on the water surface. This monolayer was again compressed to the surface pressure of 20 mN m^{-1}, at which the lithium 10,12-heptacosadiynoate monolayer was confirmed to be morphologically homogeneous. The monolayer con-

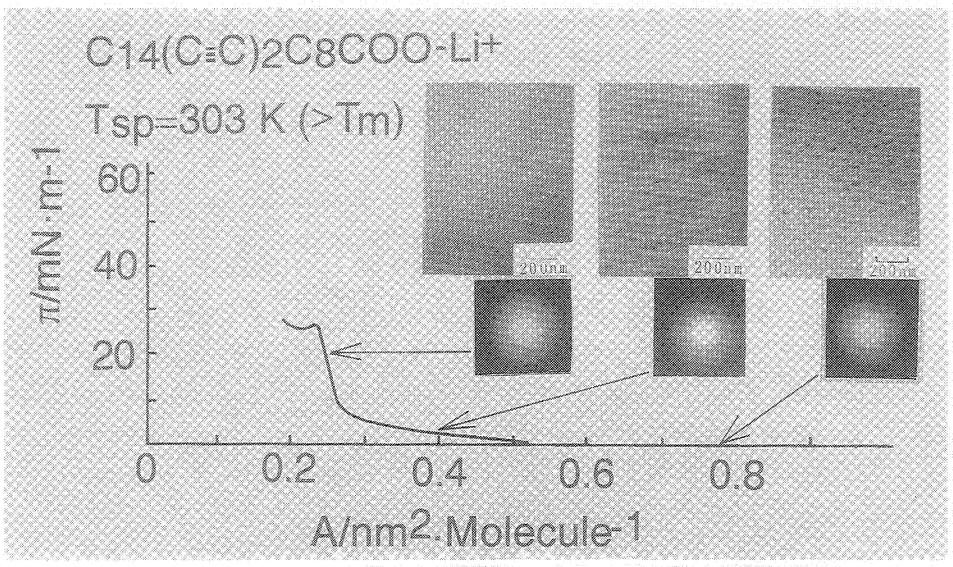

Fig. 4. Π–A isotherm, electron micrographs and ED patterns of lithium heptacosadiynoate monolayer at T_{sp} of 303 K.

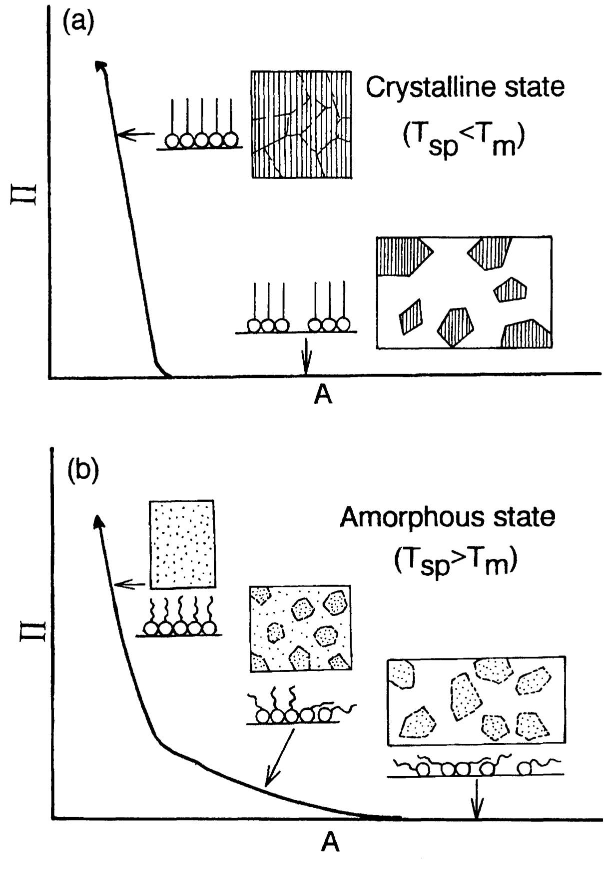

Fig. 5. Schematic representation for the molecular aggregating process of (a) crystalline monolayer and (b) amorphous monolayer.

structed by this method was designated the cooling-crystallized monolayer. In order to compare the crystallographical distortion and continuity of the cooling-crystallized monolayer with those of the crystalline monolayer, the crystalline monolayer was prepared at T_{sp} of 293 K below T_{m} and also, at a surface pressure of 20 mN m^{-1}. Crystallographical distortion and continuity in a direction along the monolayer surface were quantitatively evaluated by a modified single line method based on the Fourier analysis of ED profiles.[20,23]

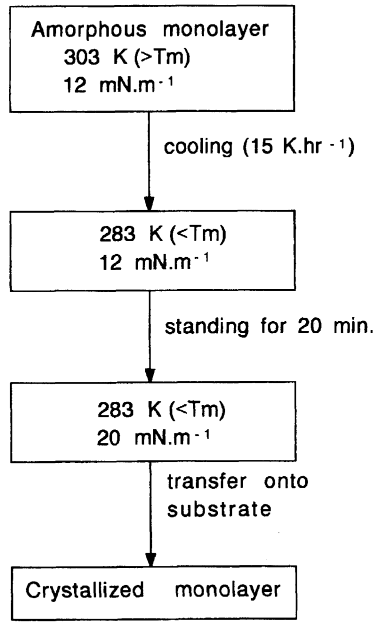

Fig. 6. Flow sheet describing the construction for crystallized monolayer.

Table 1 shows the values of crystallographical distortion and continuity for the crystalline and the cooling-crystallized monolayers of lithium 10,12-heptacosadiynoate as well as those for polyethylene single crystal. The magnitudes of crystallographical distortion and continuity for the cooling-crystallized monolayer were much smaller and larger than those for the crystalline monolayer, respectively. Furthermore, it can be considered that the crystallographical quality characteristic of the cooling-crystallized monolayer is com-

Table 1. Crystallographical Distortion and Continuity for Crystalline and Cooling-Crystallized Monolayer

	Crystallographical distortion, D_{lat} (%)	Crystallographical continuity, L_{lat} (nm)
Crystalline monolayer	6.7	1.8
Cooling-crystallized monolayer	3.1	20.4
Polyethylene (single crystal)	<2.8	>25

parable with that of high density polyethylene single crystal which was prepared under suitable conditions of crystallization as shown in Table 1. Therefore, it is clear that the monolayer of lithium 10,12-heptacosadiynoate with crystallographically superior quality can be constructed by cooling-crystallization of the amorphous monolayer on the water surface. On the other hand, in the case of the crystalline monolayer, crystallographical sintering (fusion) at the boundary surfaces among crystallites did not occur sufficiently by the compression, which suppressed the formation of the structural defect-diminished monolayer.

For the construction of PDA monolayer which has a large third order nonlinear optical susceptibility, the defect-diminished crystallized monolayer will be prepared. The details and further results of this study will be published elsewhere.

Conclusion

The melting temperature (T_{m}) of lithium 10,12-heptacosadiynoate monolayer on the water surface was evaluated to be 300 K from the subphase temperature, T_{sp} dependences of modulus and ED pattern of the monolayer which was transferred onto a hydrophilic surface. The formation of crystalline or amorphous monolayer is determined by the relative magnitude of T_{sp} to T_{m} of the monolayer, being irrespective of the surface pressure. No transition from an amorphous phase to a crystalline one was observed upon compression of the amorphous monolayer on the water surface. Furthermore, the monolayer with crystallographically superior quality could be constructed by cooling-crystallization of the amorphous monolayer on the water surface.

References

1) T. Kobayashi, "Nonlinear Optics and Semiconductors," Springer-Verlag, Berlin (1989).
2) K. C. Rustagi and J. Ducing, *Opt. Commun.*, **10**, 258 (1974).
3) C. Cojan, G. P. Agrawal, and C. Flytzanis, *Phys. Rev. Sect. B*, **B15**, 909 (1977).
4) G. P. Agrawal, C. Cojan, and C. Flytzanis, *Phys. Rev. Sect. B*, **B17**, 776 (1978).
5) G. Wegner, *Pure Appl. Chem.*, **49**, 443 (1977).
6) T. Kajiyama, K. Umemura, M. Uchida, Y. Oishi, and R. Takei, *Chem. Lett.*, **1989**, 1515.
7) Y. Tomioka, N. Tanaka, and S. Imazeki, *J. Chem. Phys.*, **91**, 5694 (1989).
8) K. Ogawa, *J. Phys. Chem.*, **95**, 7109 (1991).
9) B. Tieke and G. Lieser, *J. Colloid Interface Sci.*, **88**, 471 (1982).
10) D. Day and H. Ringsdorf, *J. Polym. Sci., Polym. Lett. Ed.*, **16**, 205 (1978).
11) N. Mino, H. Tamura, and K. Ogawa, *Langmuir*, **8**, 594 (1992).
12) T. Kajiyama, Y. Oishi, M. Uchida, N. Morotomi, J. Ishikawa, and Y. Tanimoto, *Bull. Chem. Soc. Jpn.*, **65**, 864 (1992).
13) D. Day and J. B. Lando, *Macromolecules*, **13**, 1478 and 1483 (1980).
14) K. Miyano and A. Mori, *Thin Solid Films*, **168**, 141 (1989).
15) T. Kajiyama, N. Morotomi, M. Uchida, and Y. Oishi, *Chem. Lett.*, **1989**, 1047.
16) Y. L. Chen, M. Sano, M. Kawaguchi, H. Yu, and G. Zografi, *Langmuir*, **2**, 349 (1986).
17) J. Ishikawa, M. Uchida, Y. Oishi, and T. Kajiyama, *Rep. Prog. Polym. Phys. Jpn.*, **33**, 235 (1990).
18) I. Langmuir and V. J. Schaefer, *J. Am. Chem. Soc.*, **60**, 1351 (1938).
19) K. Fukuda, H. Nakahara, and T. Kato, *J. Colloid Interface Sci.*, **54**, 430 (1976).
20) D. Hofmann and E. Walenta, *Polymer*, **28**, 1271 (1987).
21) T. Kuri, Y. Oishi, and T. Kajiyama, *Rep. Prog. Polym. Phys. Jpn.*, **35**, 347 (1992).
22) T. Kajiyama, Y. Oishi, M. Uchida, Y. Tanimoto, and H. Kozuru, *Langmuir*, **8**, 1563 (1992).
23) T. Kajiyama, I. Hanada, K. Shuto, and Y. Oishi, *Chem. Lett.*, **1989**, 193.